[redacted]

Copy
RM L9H26

NACA

RESEARCH MEMORANDUM

CONTROL EFFECTIVENESS AND HINGE-MOMENT CHARACTERISTICS OF A TIP CONTROL SURFACE ON A LOW-ASPECT-RATIO POINTED WING AT A MACH NUMBER OF 1.9

By D. William Conner and Ellery B. May, Jr.

Langley Aeronautical Laboratory
Langley Air Force Base, Va.

NATIONAL ADVISORY COMMITTEE FOR AERONAUTICS

WASHINGTON
October 5, 1949

[redacted]AL

Classification cancelled (or changed to) Unclassified

By Authority of NASA Tech Pub Announcement #103

(OFFICER AUTHORIZED TO CHANGE)

By 21 Aug 56

NSD

GRADE OF OFFICER MAKING CHANGE)

5 April 61

DATE

NACA RM L9H26

NATIONAL ADVISORY COMMITTEE FOR AERONAUTICS

RESEARCH MEMORANDUM

CONTROL EFFECTIVENESS AND HINGE-MOMENT CHARACTERISTICS OF A TIP CONTROL SURFACE ON A LOW-ASPECT-RATIO POINTED WING AT A MACH NUMBER OF 1.9

By D. William Conner and Ellery B. May, Jr.

SUMMARY

A wind-tunnel investigation was carried out on a semispan pointed wing of aspect ratio 1.7 having 60° leading-edge sweepback and 30° trailing-edge sweepforward. A control surface located at the wing tip was hinged about an axis perpendicular to the streamwise parting line separating the control. In addition to determining the characteristics of the complete configuration, normal force and hinge moment were measured on just the control surface. The test Reynolds number was 4,900,000 and the free-stream Mach number was 1.9.

The experimental rolling effectiveness of the control surface amounted to about 85 percent of that calculated by linearized theory. With the use of experimental data the effects of wing trailing-edge sweepforward on roll control in free flight were calculated. For configurations having equal lift effectiveness and the same area tip-control surfaces, about one-fourth more roll control would be developed by the sweptforward trailing-edge arrangement than by an unswept arrangement because of a lower wing damping moment and because of increased rolling-moment effectiveness. At zero angle of attack the normal-force and hinge-moment variations with deflection were reasonably well predicted by linearized theory. At low angles of attack the control-surface hinge moment exhibited nonlinear variations with control deflection and with angle of attack. No significant changes in the characteristics of either the complete wing or of the control surface were experienced when the gap width at the parting line separating the control from the inner wing panel was increased from about 0 to 1.4 percent of the local wing chord.

INTRODUCTION

Free-flight rocket tests have indicated that flap-type controls often have serious reductions or reversals in lateral control effectiveness at transonic and supersonic speeds, whereas full-chord tip controls maintain satisfactory control effectiveness in these speed ranges (reference 1). Because of the general interest in such full-chord controls, wind-tunnel investigations of two wing-control configurations have been made. Reference 2 reports the characteristics at a Mach number of 1.9 of a half-delta control comprising the outer one-third of a 60° sweptback semispan delta wing. The tests presented herein are an extension of this tunnel program and report the characteristics of a different plan-form wing-tip control combination.

The wing of pointed plan form had 60° leading-edge sweepback and 30° trailing-edge sweepforward, and a control surface comprised the outer 28 percent of the exposed-wing semispan. Force and moment measurements were obtained for the wing in the presence of a fuselage through a range of control deflections and a small range of angles of attack. Normal force and hinge moment were measured on the control. Various gaps were tried between the control root chord and inner wing panel. The results have been correlated with the results of reference 2 to show the effects of wing trailing edge sweepforward on roll control in free flight.

COEFFICIENTS AND SYMBOLS

C_L	lift coefficient $\left(\frac{\text{Lift}}{qS}\right)$
C_D	drag coefficient $\left(\frac{\text{Drag}}{qS}\right)$
C_m	pitching-moment coefficient $\left(\frac{M'}{qS\bar{c}}\right)$
C_l	rolling-moment coefficient $\left(\frac{L}{2qSb}\right)$
C_n	yawing-moment coefficient $\left(\frac{N}{2qSb}\right)$
M'	pitching moment about center of area of exposed wing
L	rolling moment about axis of fuselage

N yawing moment about an axis perpendicular to fuselage center line

$$C_{N_f} = \frac{N_f}{qS_f}$$

$$C_{m_f} = \frac{M_f}{qS_f\bar{c}_f}$$

N_f control-surface force normal to control-surface chord plane

M_f control-surface pitching moment (hinge moment) about control-surface pivot axis

q free-stream dynamic pressure

S exposed semispan wing area (22.2 sq in.)

$\bar{c}$ mean aerodynamic chord of exposed-wing area (6.72 in.)

b twice the distance from the fuselage axis to wing tip (10.40 in.)

S_f control-surface area (1.66 sq in.)

$\bar{c}_f$ mean aerodynamic chord of control surface (1.847 in.)

α angle of attack of wing chord plane measured with respect to free-stream direction

δ control-surface deflection measured with respect to wing chord plane in free-stream direction

R Reynolds number based on $\bar{c}$

M Mach number

MODEL

The system of axes is shown in figure 1. A photograph of the semispan model mounted in the test section is shown in figure 2, and the principal dimensions are shown in figure 3.

The triangular-plan-form wing panel had a leading-edge sweepback angle of 60° and trailing-edge sweepforward angle of 30°. The aspect

[redacted]

ratio of the wing was 1.7 when the leading and trailing edges were considered to extend to the fuselage center line.

The inner wing panel was a modified version of the panel used in the tests of reference 2. The modification consisted of a triangular addition to the trailing edge which resulted in a sweptforward trailing edge. (See fig. 2.) The airfoil sections of the inner panel were hexagonal in shape, formed from an untapered flat plate, and were 2.5 percent thick at the fuselage intersection and 9 percent thick at the outboard end. The leading-edge wedge had an included wedge angle of 6.6° measured parallel to the air stream. The leading-edge wedge was modified by a small nose radius, and the sharp breaks in contour were modified by a slight fairing.

The control surface which made up the outer portion of the wing was separated from the inner wing panel by a streamwise parting line and rotated about an axis perpendicular to the root chord. The axis was located at 63 percent of the control-surface root chord and was $0.075\bar{c}_f$ behind the center of area of the control. Since the control was comprised of 3-percent-thick airfoil sections, a discontinuity in thickness existed at the parting line separating the control surface and main panel.

All tests of the wing and of the control surface were made in the presence of a half-fuselage. The nose section of the fuselage (a body of revolution) merged into a constant-diameter section at the station where the wing leading edge intersected the fuselage.

TUNNEL AND TEST TECHNIQUE

The Langley 9- by 12-inch supersonic blowdown tunnel in which the present tests were made is a nonreturn-type tunnel utilizing the exhaust air from the Langley 19-foot pressure tunnel. The air enters at an absolute pressure of about $2\frac{1}{3}$ atmospheres and contains about 0.3 percent of water by weight.

The model arrangement was similar to that used in the tests of reference 2. The semispan models are cantilevered from a five-component strain-gage balance mounted flush with the tunnel wall. The balance and fuselage rotate with the wing as the angle of attack is changed, and the forces and moments are measured with respect to the balance axes. The balance was used to measure the normal force and pitching moment of the control surface in the presence of the inner wing panel. The semispan wing model was tested in the presence of, but not attached to, a half-fuselage (reference 3).

The dynamic pressure and test Reynolds number decreased about 5 percent during the course of each run because of the decreased pressure of the inlet air. The average dynamic pressure was 11.8 pounds per square inch and the average Reynolds number, based on the mean aerodynamic chord of the exposed wing, was 4.9×10^6.

PRECISION OF DATA

The free-stream Mach number has been calibrated at 1.90 ±0.02. This Mach number was used in determining the dynamic pressure. Calibration tests made with the tunnel clear in the space normally occupied by the model and extending about 4 inches ahead of the wing reference axis and outside the wall boundary layer indicated that the static pressure varied about ±1.5 percent from a mean value. A discussion is given in reference 3 of the various factors which might influence the test results, such as humidity effects and method of mounting.

An estimate has been made of the probable errors to be found in the measured test points, when fluctuations in the readings of the measuring equipment, calibration errors, and shift of instrument no-load readings experienced during the course of each test are considered. The following table lists the errors that might be expected to exist between the test points for each particular figure.

Wing		Control surface	
Variable	Error	Variable	Error
α	±0.05°	α	±0.05°
δ	±.2°	δ	±.2°
C_L	±.003	C_{N_f}	±.005
C_D	±.001	C_{m_f}	±.008
C_m	±.001		
C_l	±.0004		
C_n	±.0003		

[redacted]

Static calibration indicated that the angular deflection of the control caused by control hinge moment was negligible.

RESULTS AND DISCUSSION

Wing Characteristics

Figure 4 presents the wing test data for the range of control deflections and parting-line gaps tested. Within the experimental accuracy there were no changes in the aerodynamic characteristics of the wing caused by change in gap width at the parting line.

The experimental lift-curve slope for the wing was 0.039 which equalled the theoretical value for a wing of this plan form. The theoretical value, however, did not include fuselage upwash effects which would be estimated to increase the slope by the order of 20 percent for this arrangement at this Mach number. Using the lift and moment curves of figure 4, the center of pressure at zero control deflection was calculated to be located $0.064\bar{c}$ ahead of the center of area and 37 percent of the exposed-wing semispan outboard of the fuselage intersection. Neglecting upwash effects, theory indicates the spanwise center of pressure to be located at the 41.6-percent station of the exposed-wing semispan.

The curves of figure 4 have been cross-plotted in figure 5 to show the variation of the coefficients with control deflection for zero angle of attack. This figure also includes the characteristics calculated from linearized theory (reference 4). In applying the theory to this plan form which has a swept trailing edge, recourse was taken to a graphic method for integrating the loading in the region behind the station of maximum span. The experimental lift effectiveness of the flap was less than that calculated. The experimental rolling effectiveness $\frac{dC_l}{d\delta}$ of 0.00061 was about 15 percent less than the calculated value of 0.00072. The following table is presented to better illustrate the roll-control characteristics of this model as compared with the results obtained in tests of a 60° delta wing with tip control (reference 2).

	Test model	Model of reference 2
Sweep angle of wing trailing edge, degrees	−30	0
Ratio of control area in percent of exposed-wing area	7.6	10.8
Experimental $\frac{dC_l}{d\delta}$	0.00061	0.00075
Theoretical damping coefficient (C_{l_p}) of plain wing (reference 5)	−.174	−.197
Experimental lift-curve slope $\frac{dC_L}{d\alpha}$	0.039	0.040

The spanwise center of pressure of the control-surface loading (in percent control span) can be considered to be independent of the size of the control surface relative to the wing size. Such a consideration makes possible a comparison of the roll effectiveness of tip-control surfaces on the two different plan-form wings by adjusting the relative size of the control surfaces. Two different bases of comparison are used. In the first case, the control-surface area is considered to be a given constant percentage of the exposed-wing area. In the second case, the control-surface areas are considered to be equal, but the wing areas differ so that a constant value results from the product of the wing lift-curve slope and the wing area. The wings then have equal lift effectiveness at any angle of attack. In both cases the comparisons are for the calculated rate of roll (wing-tip helix angle per unit control deflection) which would be experienced in free flight. The wing-tip helix angle equals the rolling-effectiveness parameter $\frac{dC_l}{d\delta}$ divided by the damping-in-roll coefficient C_{l_p}. Experimental damping-in-roll coefficients are not available at the Mach number under consideration. Theoretical values for the wings alone, therefore, were calculated (reference 5) and are used to establish an approximate relation between the free-flight roll control of the two configurations.

In the case of equal percentage control areas, increasing the area of the test model to 10.8 percent of the wing area by moving the parting line inboard would increase the value of $\frac{dC_l}{d\delta}$ from 0.00061 to 0.00083,

[redacted]

a value 10.7 percent greater than that measured on the delta wing of reference 2. The calculated free-flight roll control would be 25.3 percent greater for the test model arrangement than for the delta-wing arrangement.

In the case of wings having equal lift effectiveness and controls of the same absolute size, the control area of the delta wing (reference 2) was left unchanged at 10.8 percent of the delta-wing area. The control area would then be 10.5 percent of the area of the test model (with the sweptforward trailing edge). Based on these sizes the free-flight roll control was calculated to be 22.5 percent greater for the test model plan form than for the delta plan form.

From the analysis carried out on either basis the results were about the same; namely, the free-flight roll control of a tip-control surface on a pointed wing was about one-fourth greater when the wing trailing edge was swept forward 30°. The greater amount of roll control per unit control area results from a lower damping moment per unit wing area and from increased rolling-moment effectiveness $\frac{dC_l}{d\delta}$ per unit control area. The roll effectiveness per unit area increases because the carry-over loading of the tip control affects a much greater area of the inboard wing panel. Also, as will be pointed out later, the theoretical lift loading of the control was more nearly realized.

Control-Surface Characteristics

Figures 6 and 7 present the data for the control alone, tested in the presence of the inner wing panel and fuselage. The faired curves from figure 6 are repeated in figure 7 as dotted curves to indicate better the effects of gap at the parting line. The data of figures 6 and 7 are cross-plotted in figure 8 to show the variation of the coefficients with control deflection. Part (a) of figure 8 is for zero angle of attack and includes theoretical curves applicable for small deflections. Part (b) of figure 8 presents the data for angles of attack of 0° and 2° for the configuration with the small parting-line gap. Since the model had symmetrical airfoil sections, all angles and coefficients can arbitrarily be reversed in sign. This change in sign makes possible the application of the test data to include the condition of negative angles of deflection for the control. This procedure has been followed in presenting the data of figure 8(b) to show the nature of the curve shapes in the negative range of control deflections. In going from negative to positive angles, a discontinuity exists in the curves as a result of inaccuracies in the test measurements.

For all deflections the normal-force coefficient varied linearly with angle of attack between C_{N_f} values of 0 and 0.2 (fig. 6(a)). At higher values of normal-force coefficient the curves tended to round off. Increasing the control deflection decreased somewhat the rate-of-change of normal-force coefficient with wing angle of attack. Increasing the gap at the parting line (fig. 7(a)) caused a slight decrease in the slope of the normal-force curve, especially for the high-load conditions. Within the experimental accuracy the normal-force coefficient varied linearly with control deflection (fig. 8). Agreement with theory for zero angle of attack was good. It should be pointed out that for the delta-wing tests (reference 2) where the conditions of leading-edge sweep, airfoil section, and parting-line gap were the same as for these tests, the theoretical normal force was not fully realized.

The hinge-moment coefficient C_{m_f} varied nonlinearly with angle of attack (fig. 6(b)) as a result of a rearward shift in center of pressure which occurred when the wing was rotated from a streamwise direction. This rearward shift also occurred in tests of the delta-wing-control combination (reference 2). Increasing the gap at the parting line caused no well-defined effects in the hinge-moment characteristics. At zero angle of attack the hinge moment increased almost linearly with control deflection at nearly the same rate as that predicted by theory. At an angle of attack of 2° the hinge moment had nonlinear variations with deflection (of greater magnitude than could be explained by experimental inaccuracies) which would complicate any attempt made to obtain a well-balanced control through relocation of the hinge line.

CONCLUSIONS

From an investigation at a Mach number of 1.9 of a low-aspect-ratio pointed wing with tip-control surface in the Langley 9- by 12-inch supersonic blowdown tunnel, the following conclusions may be drawn:

1. The experimental rolling effectiveness of the control surface amounted to about 85 percent of that calculated by linearized theory. With the use of experimental data the effects of wing trailing-edge sweepforward on roll control in free flight were calculated. For configurations having equal lift effectiveness and the same area tip-control surfaces, about one-fourth more roll control would be developed by the sweptforward trailing-edge arrangement than by an unswept arrangement because of a lower wing damping moment and because of increased rolling-moment effectiveness.

[redacted]

2. At zero angle of attack the normal-force and hinge-moment variations with deflection were reasonably well predicted by linearized theory. At low angles of attack the control-surface hinge moment exhibited nonlinear variation with control deflection and with angle of attack.

3. No significant change in the characteristics of either the complete wing or of the control surface were experienced when the gap width at the parting line separating the control from the inner wing panel was increased from nearly 0 to 1.4 percent of the local wing chord.

Langley Aeronautical Laboratory
National Advisory Committee for Aeronautics
Langley Air Force Base, Va.

REFERENCES

1. Sandahl, Carl A.: Free-Flight Investigation of the Rolling Effectiveness of Several Delta Wing-Aileron Configurations at Transonic and Supersonic Speeds. NACA RM L8D16, 1948.

2. Conner, D. William, and May, Ellery B., Jr.: Control Effectiveness Loads and Hinge-Moment Characteristics of a Tip Control Surface on a Delta Wing at a Mach Number of 1.9. NACA RM L9H05, 1949.

3. Conner, D. William: Aerodynamic Characteristics of Two All-Movable Wings Tested in the Presence of a Fuselage at a Mach Number of 1.9. NACA RM L8H04, 1948.

4. Lagerstrom, P. A., and Graham, Martha E.: Linearized Theory of Supersonic Control Surfaces. Jour. Aero. Sci., vol. 16, no. 1, Jan. 1949, pp. 31-34.

5. Malvestuto, Frank S., Jr., and Margolis, Kenneth: Theoretical Stability Derivatives of Thin Sweptback Wings Tapered to a Point with Sweptback or Sweptforward Trailing Edges for a Limited Range of Supersonic Speeds. NACA TN 1761, 1949.

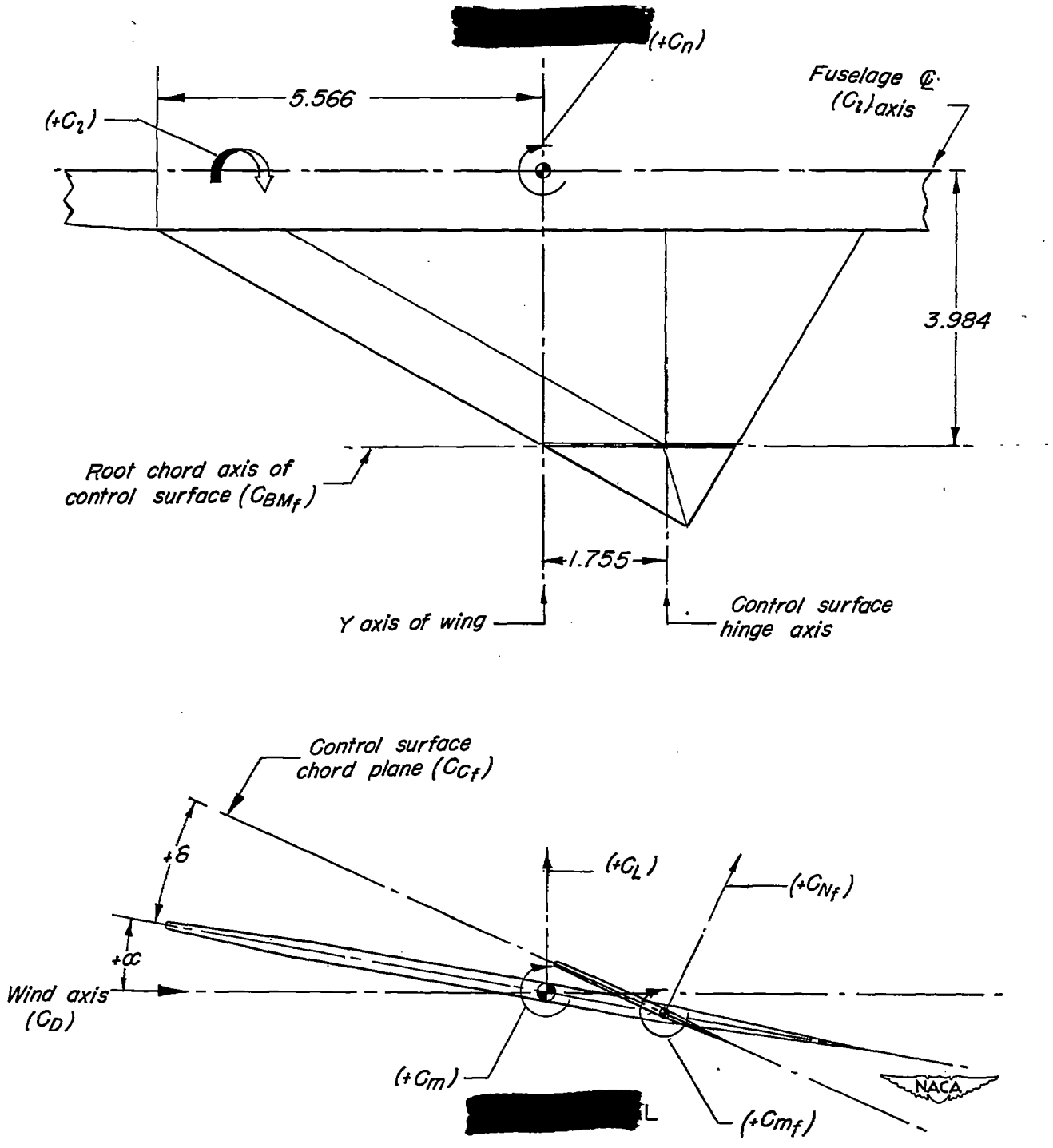

Figure 1.— Relation between the various reference axes and reference planes used in presenting test data for control surface. All dimensions in inches.

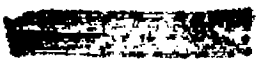

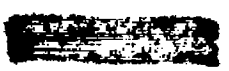

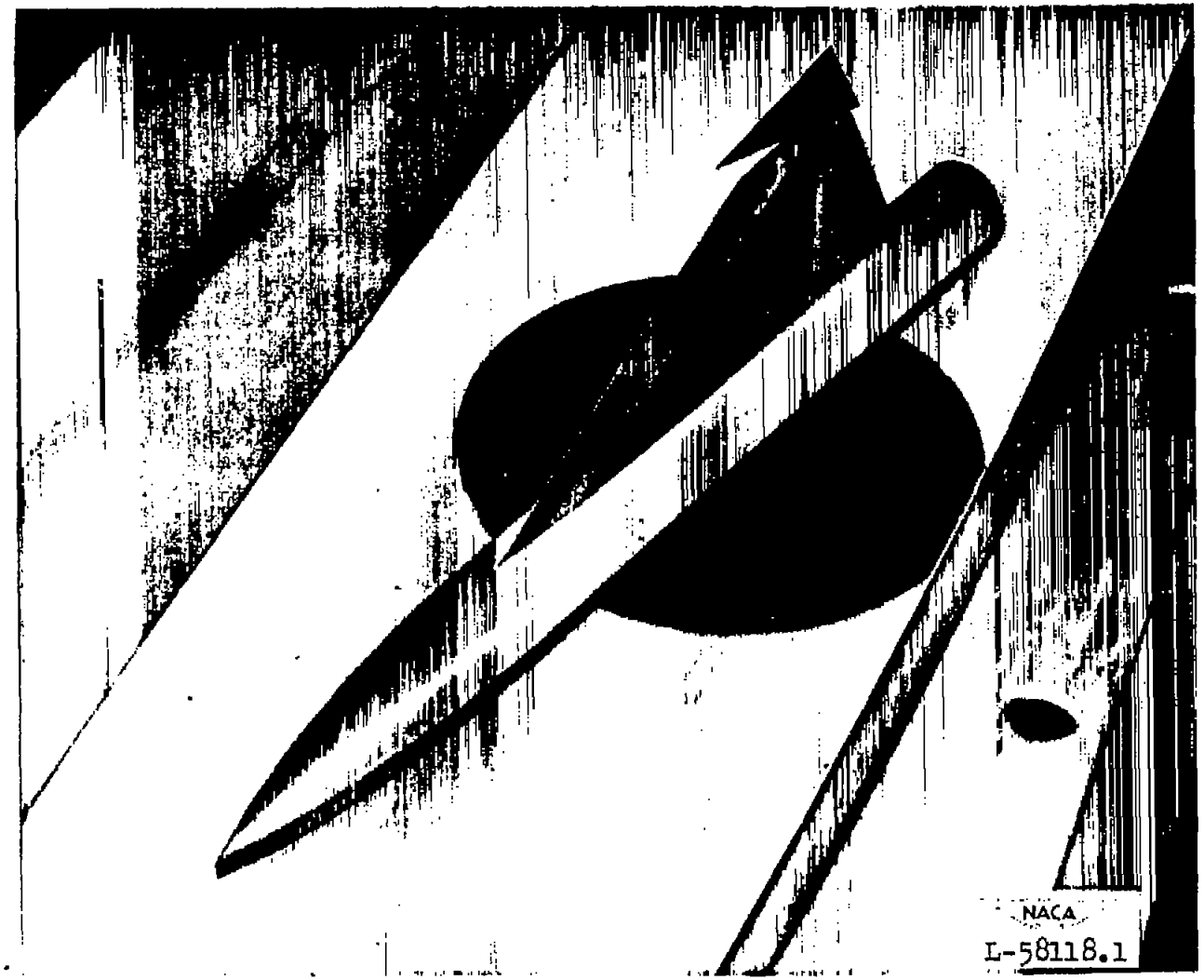

Figure 2.– Model mounted in Langley 9– by 12–inch supersonic blowdown tunnel.

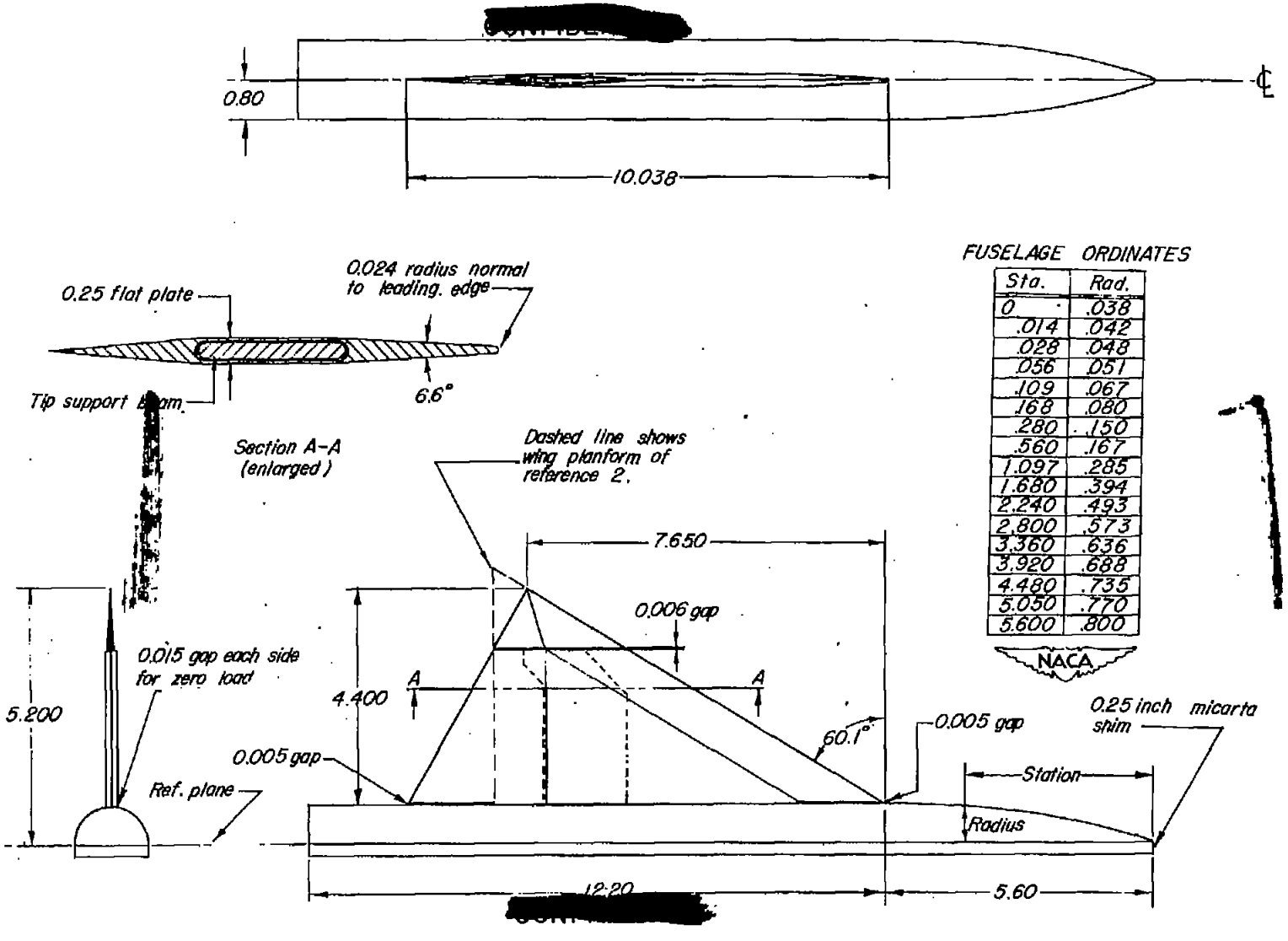

FUSELAGE ORDINATES

Sta.	Rad.
0	.038
.014	.042
.028	.048
.056	.051
.109	.067
.168	.080
.280	.150
.560	.167
1.097	.285
1.680	.394
2.240	.493
2.800	.573
3.360	.636
3.920	.688
4.480	.735
5.050	.770
5.600	.800

NACA

(a) Complete wing and fuselage; mean aerodynamic chord, 6.72; span, 10.40.

Figure 3.- Details of model. All dimensions in inches.

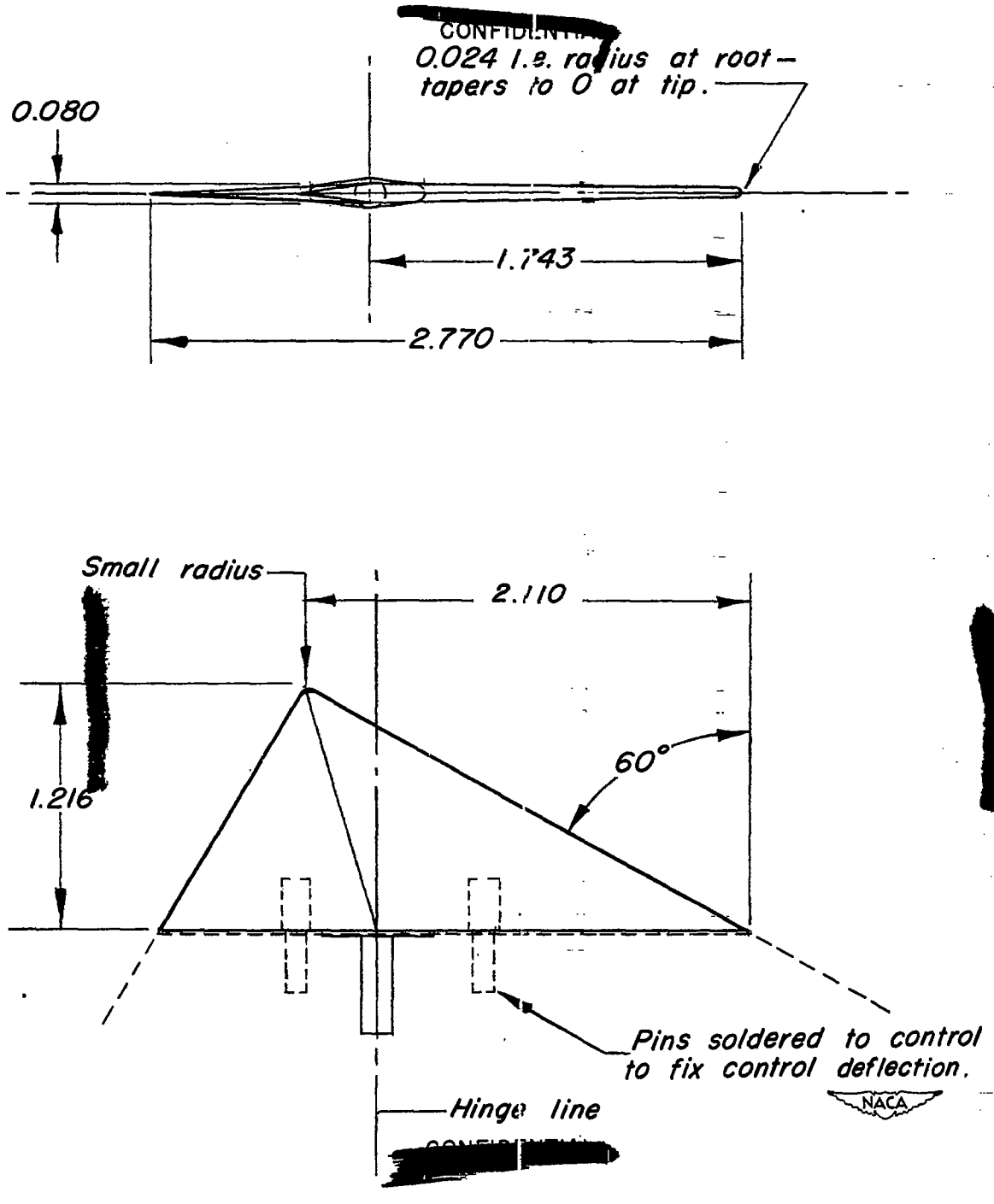

(b) Details of tip control. Mean aerodynamic chord, 1.847.

Figure 3.— Concluded.

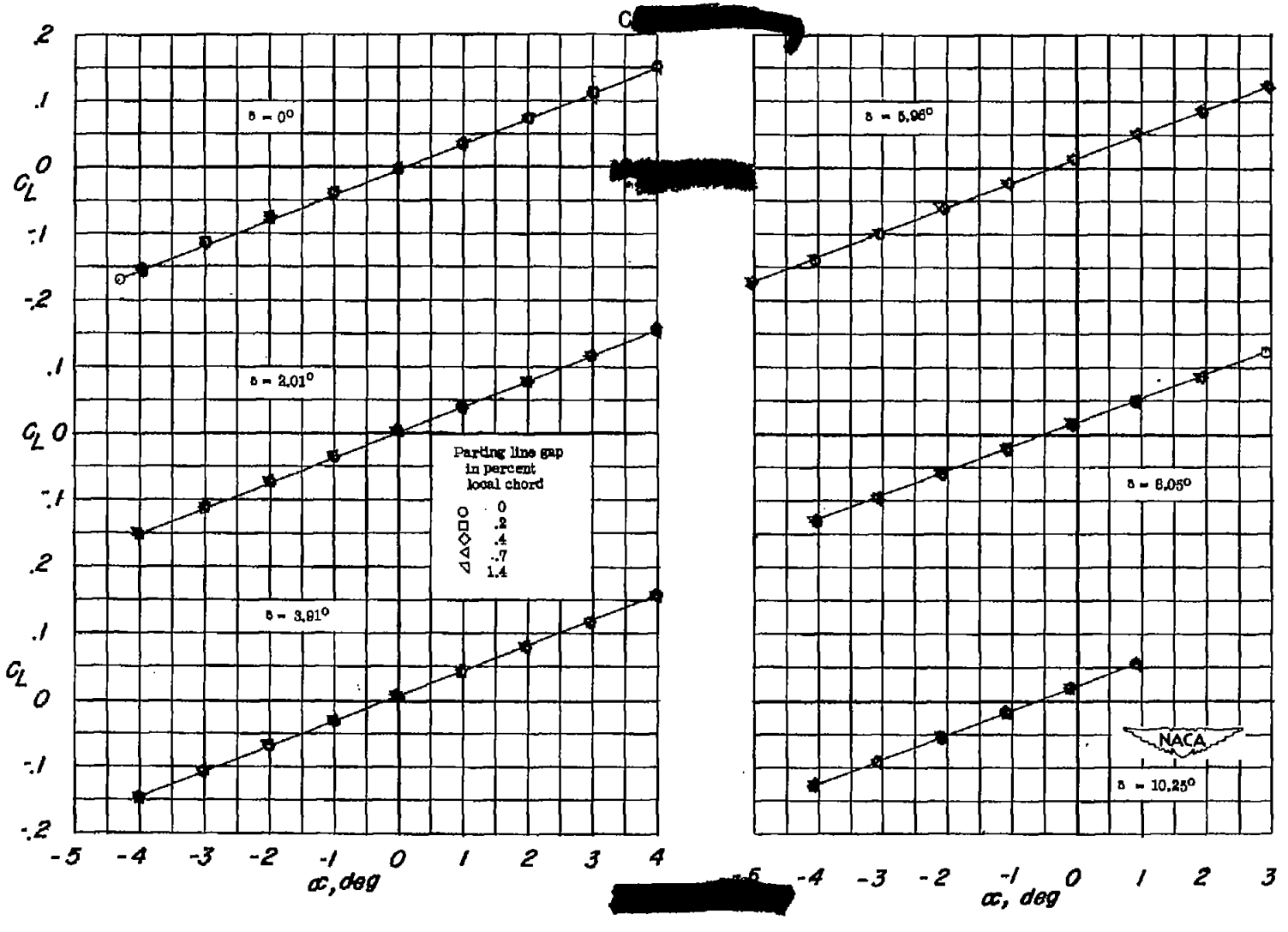

(a) Variation of lift coefficient with α.

Figure 4.– Aerodynamic characteristics of a 60° sweptback semispan pointed wing of aspect ratio 1.7 for various tip-control deflections and for [redacted] between the tip control and the main panel. M = 1.90; R = 4.9 × 10^6.

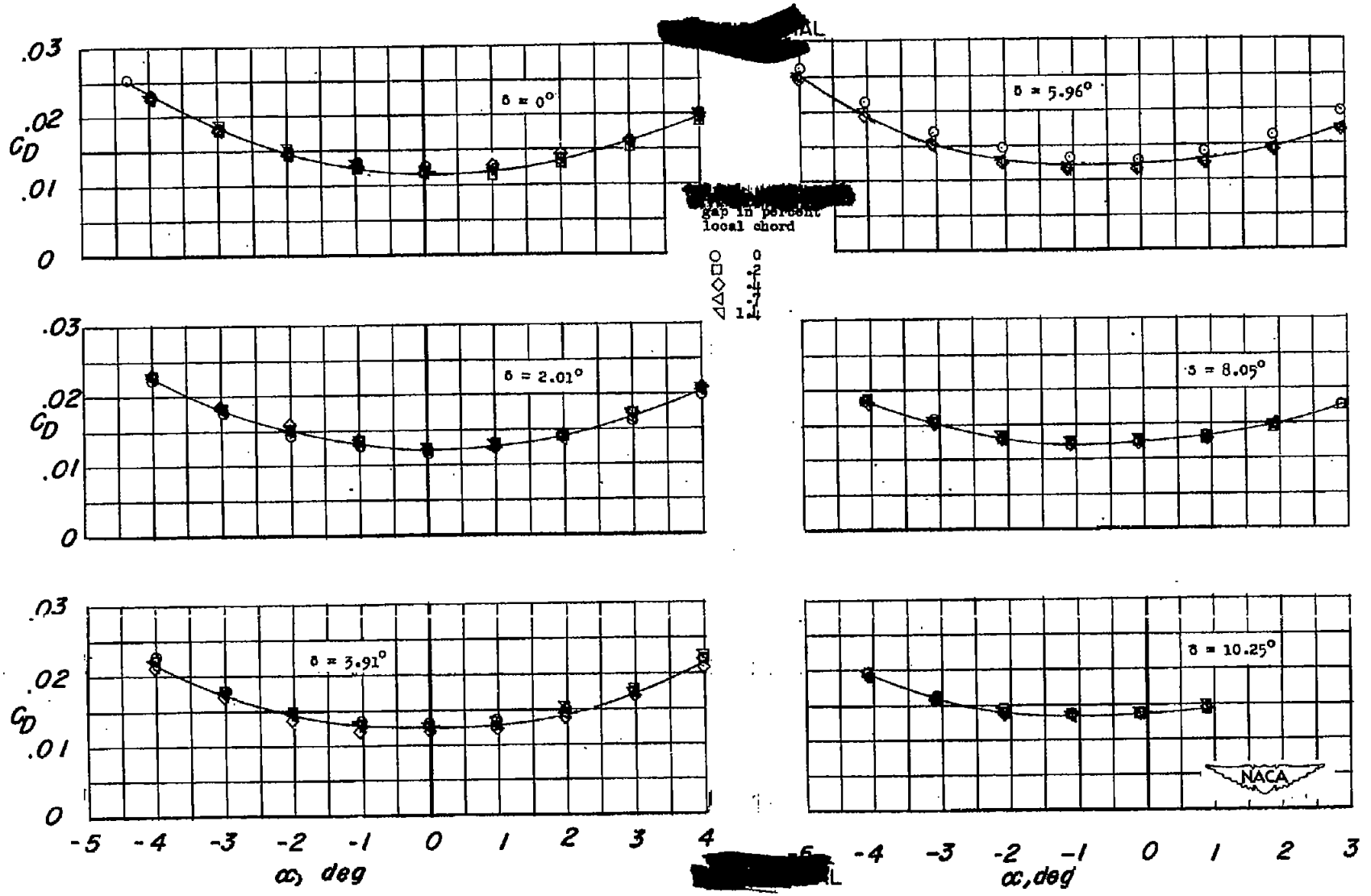

(b) Variation of drag coefficient with α.

Figure 4.— Continued

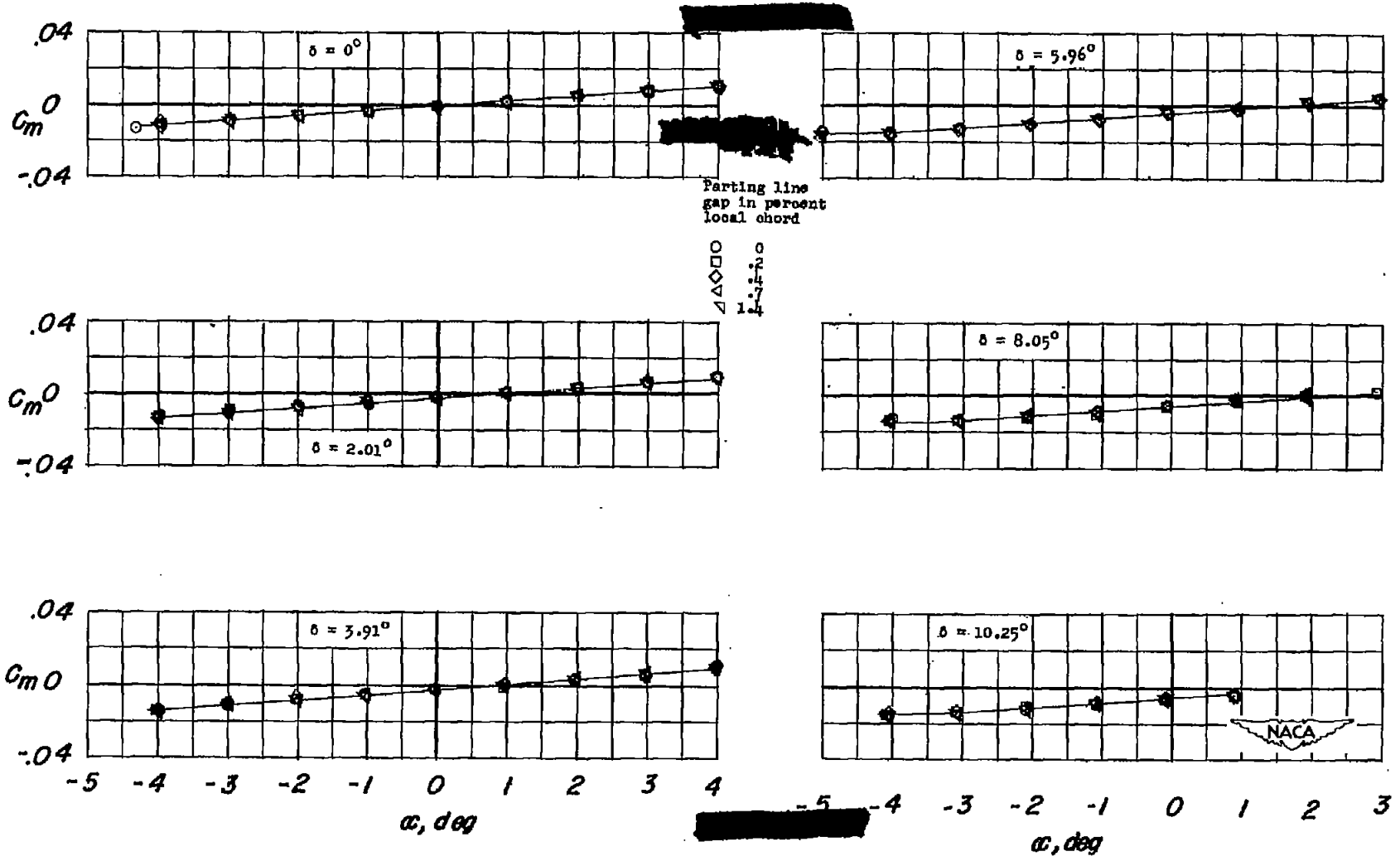

(c) Variation of pitching-moment coefficient with α.

Figure 4.– Continued.

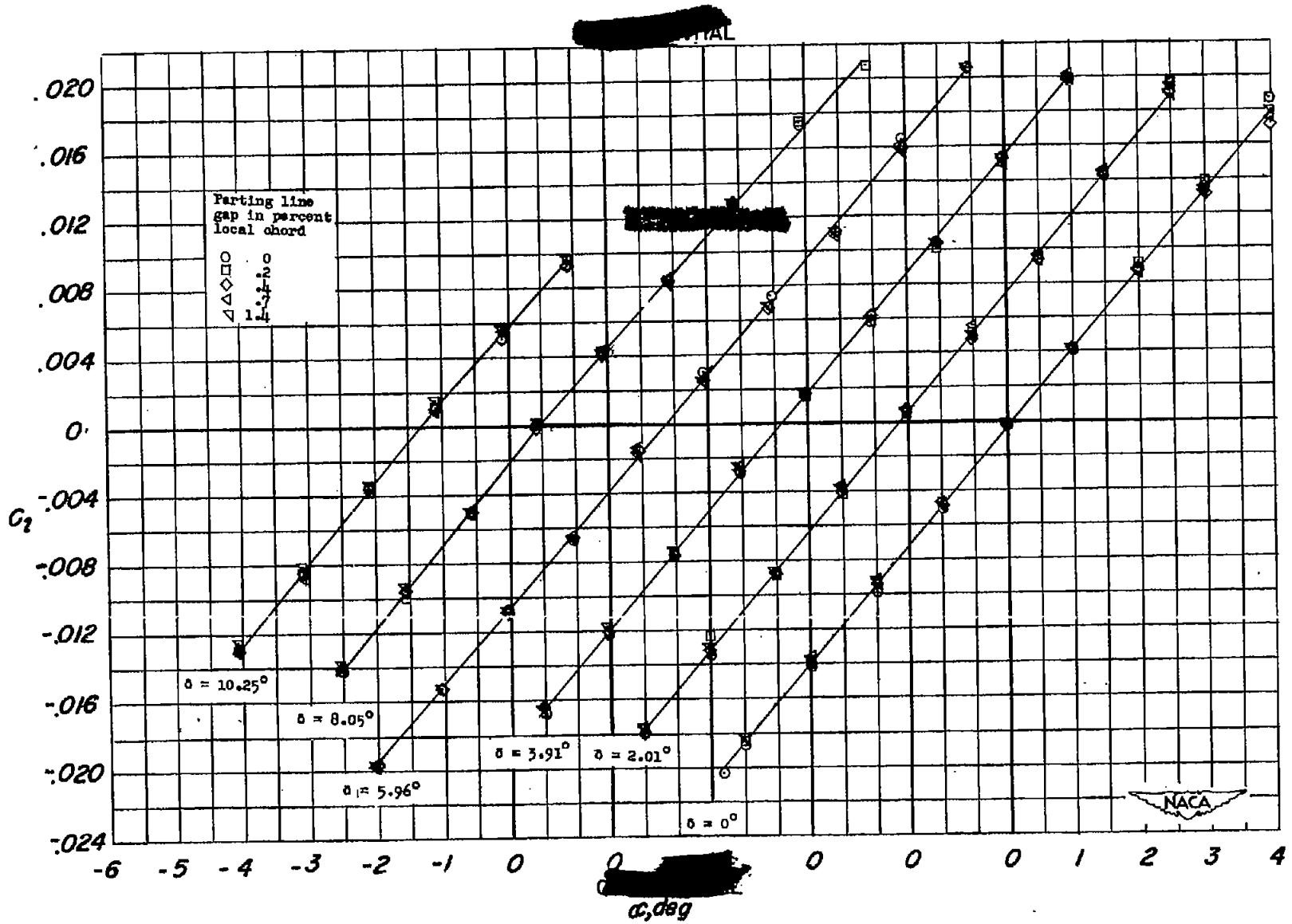

(d) Variation of rolling moment coefficient with α.

Figure 4.– Continued.

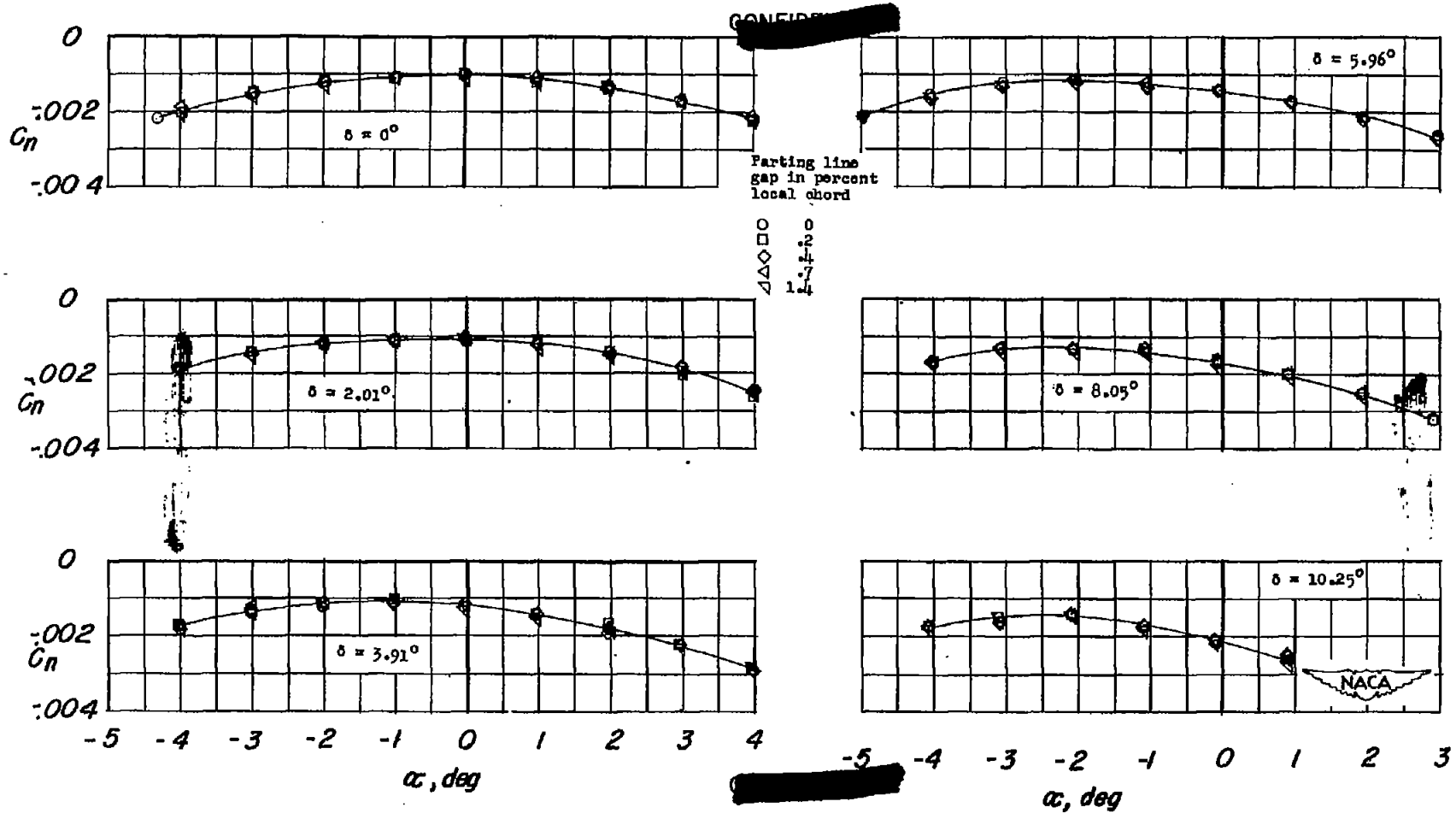

(e) Variation of yawing-moment coefficient with α.

Figure 4.– Concluded.

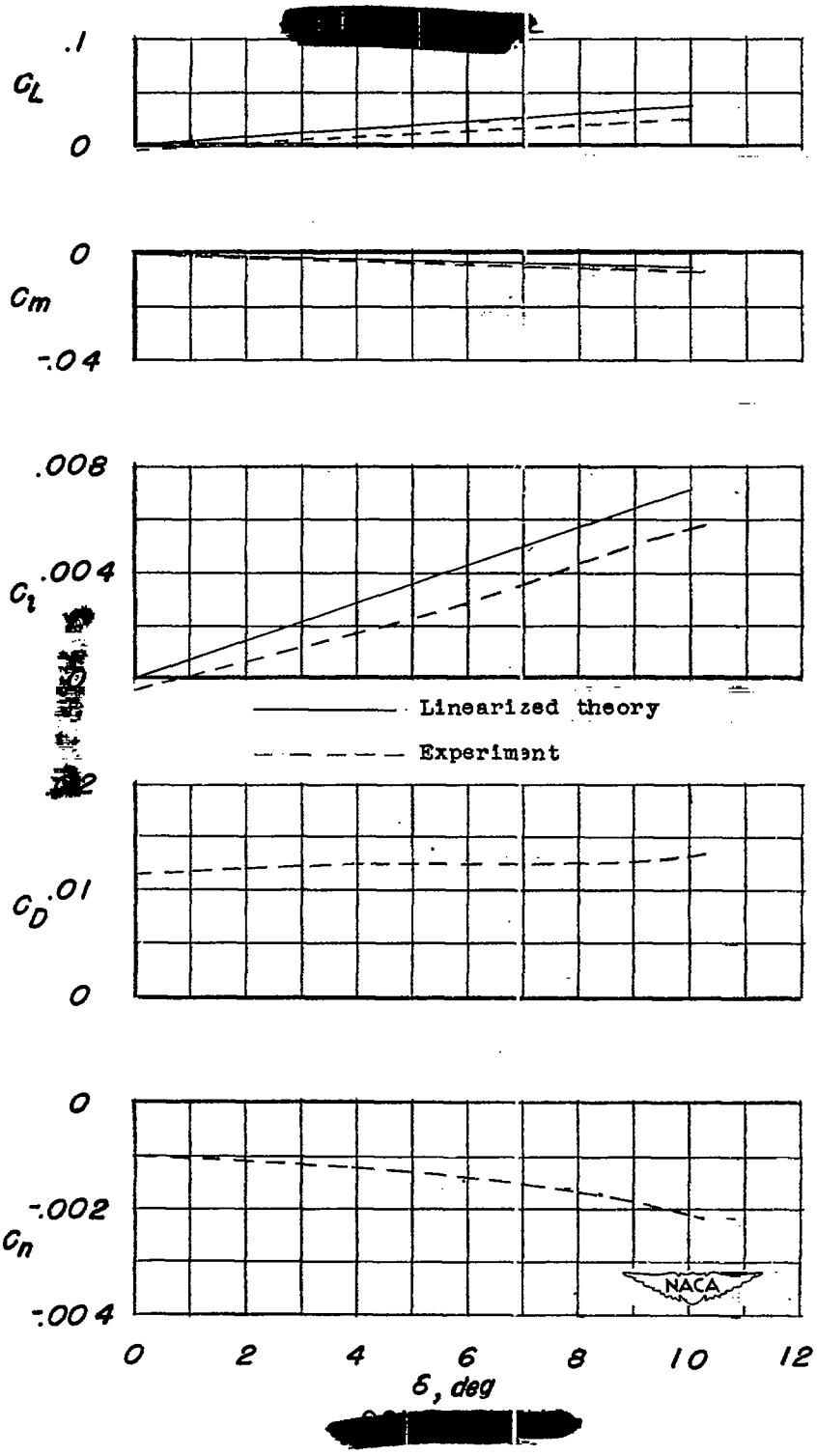

Figure 5.— Variation of the aerodynamic characteristics of a semispan pointed wing with deflection of the tip control surface. $R = 4.9 \times 10^6$; $M = 1.90$; $\alpha = 0^\circ$.

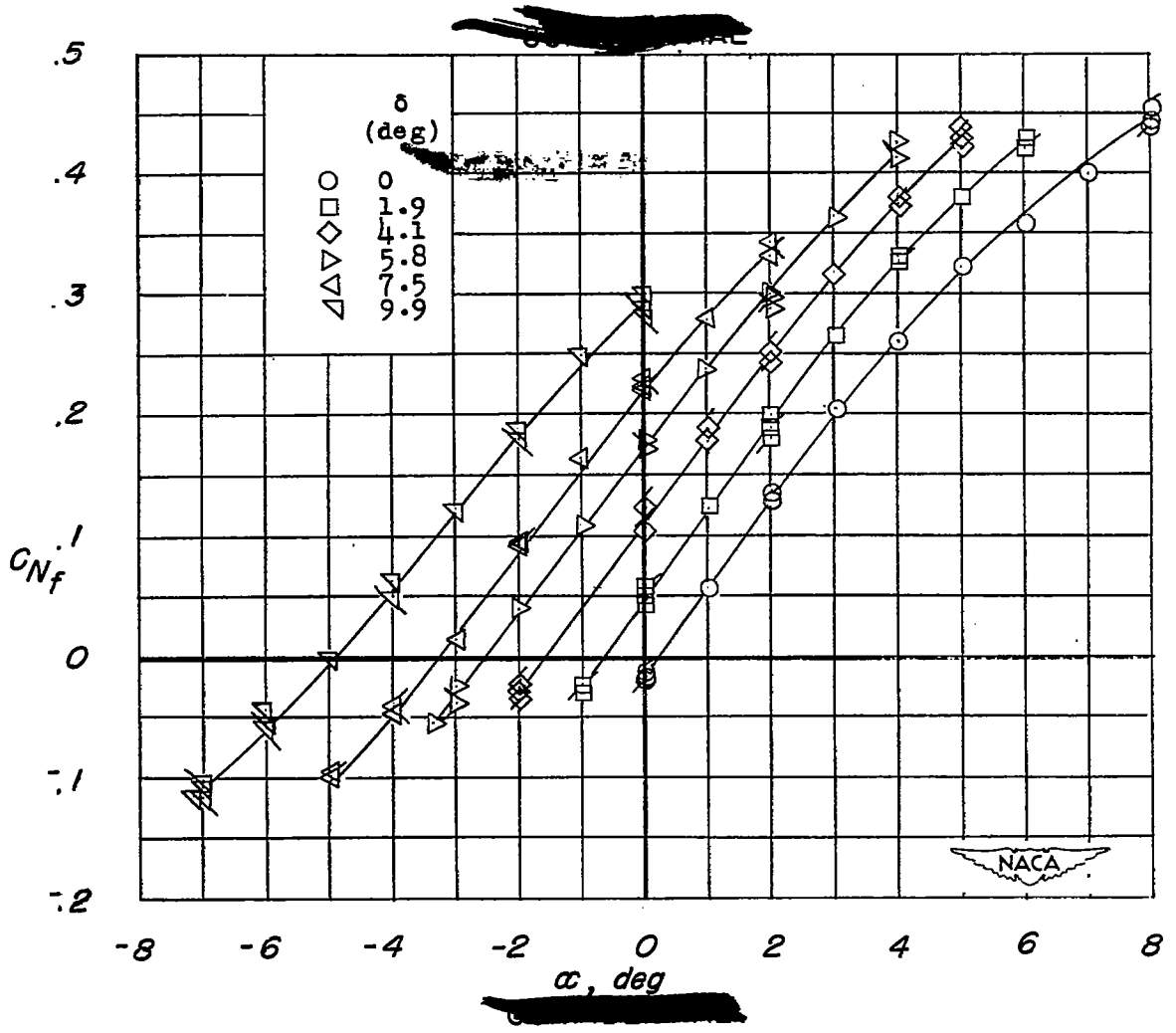

(a) C_{N_f} plotted against α.

Figure 6.— Aerodynamic loading characteristics of a tip control surface on a pointed wing. Data presented with respect to control surface axes. Parting line gap = 0.2 percent of local chord.

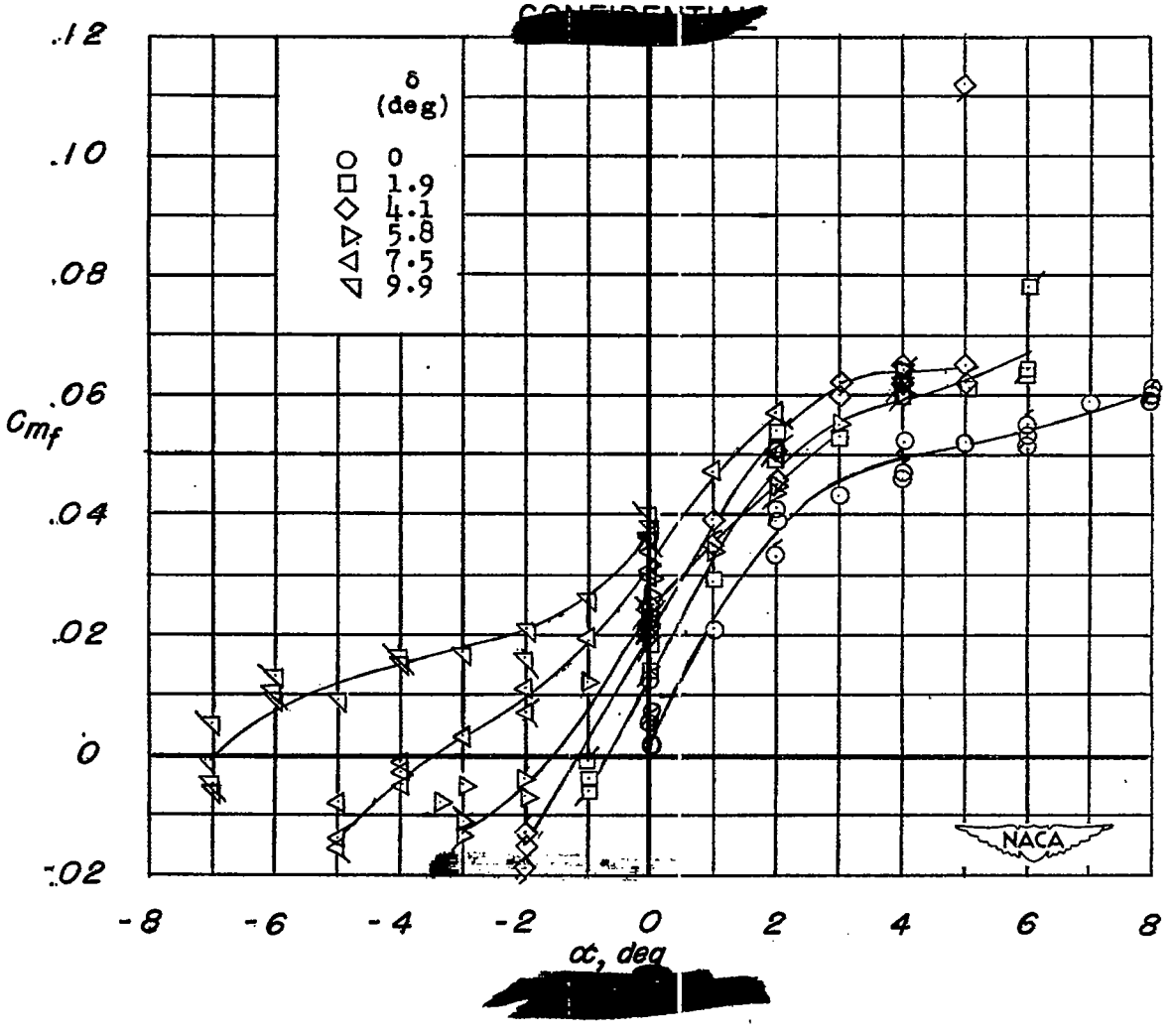

(b) C_{m_f} plotted against α.

Figure 6.– Concluded.

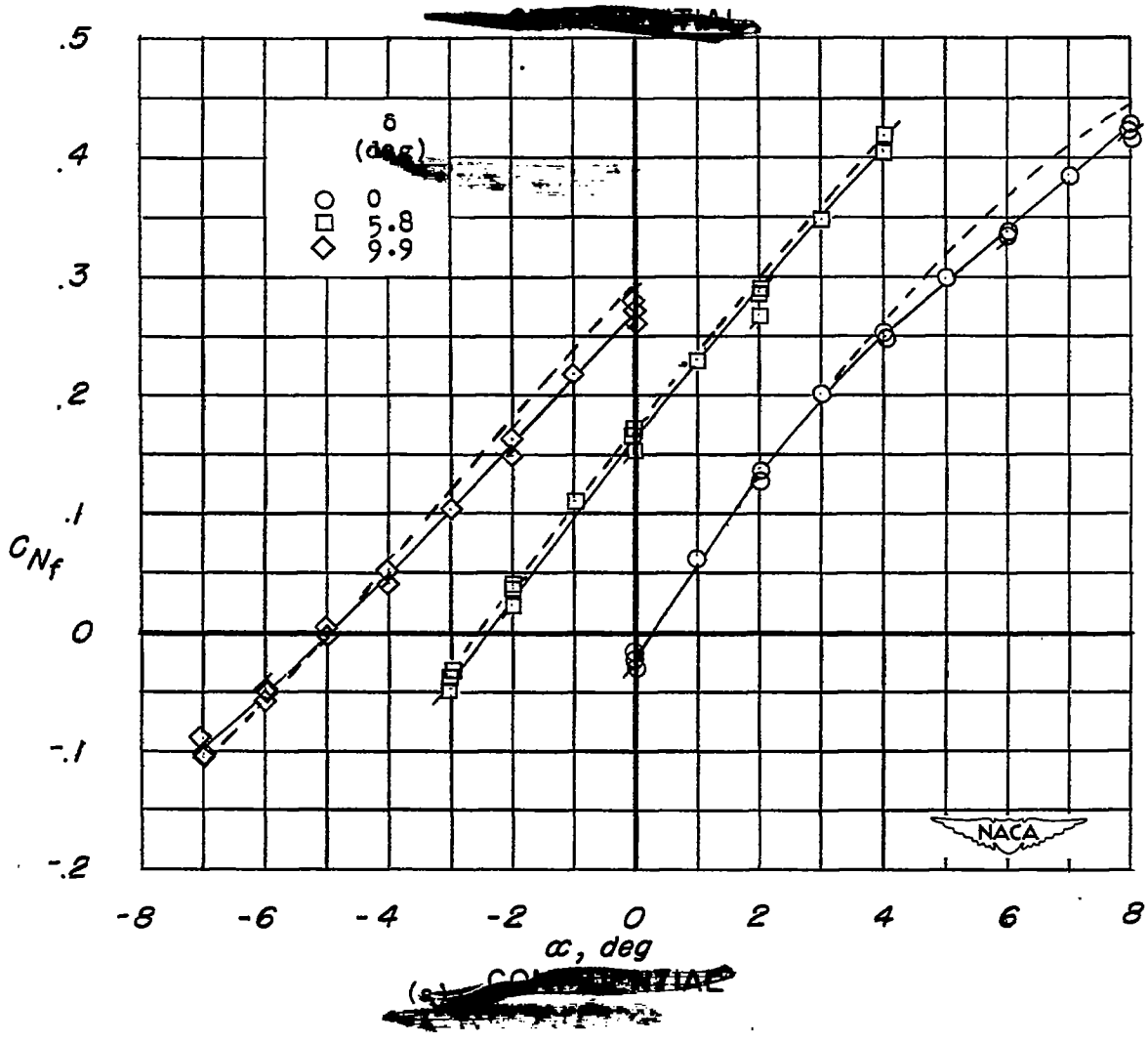

(a) C_{N_f} plotted against α.

Figure 7.— Aerodynamic loading characteristics of a tip control surface on a pointed wing. Data presented with respect to control surface axes. Parting line gap = 1.4 percent of local chord. Dotted curves are from figure 6 for parting line gap of 0.2 percent local chord.

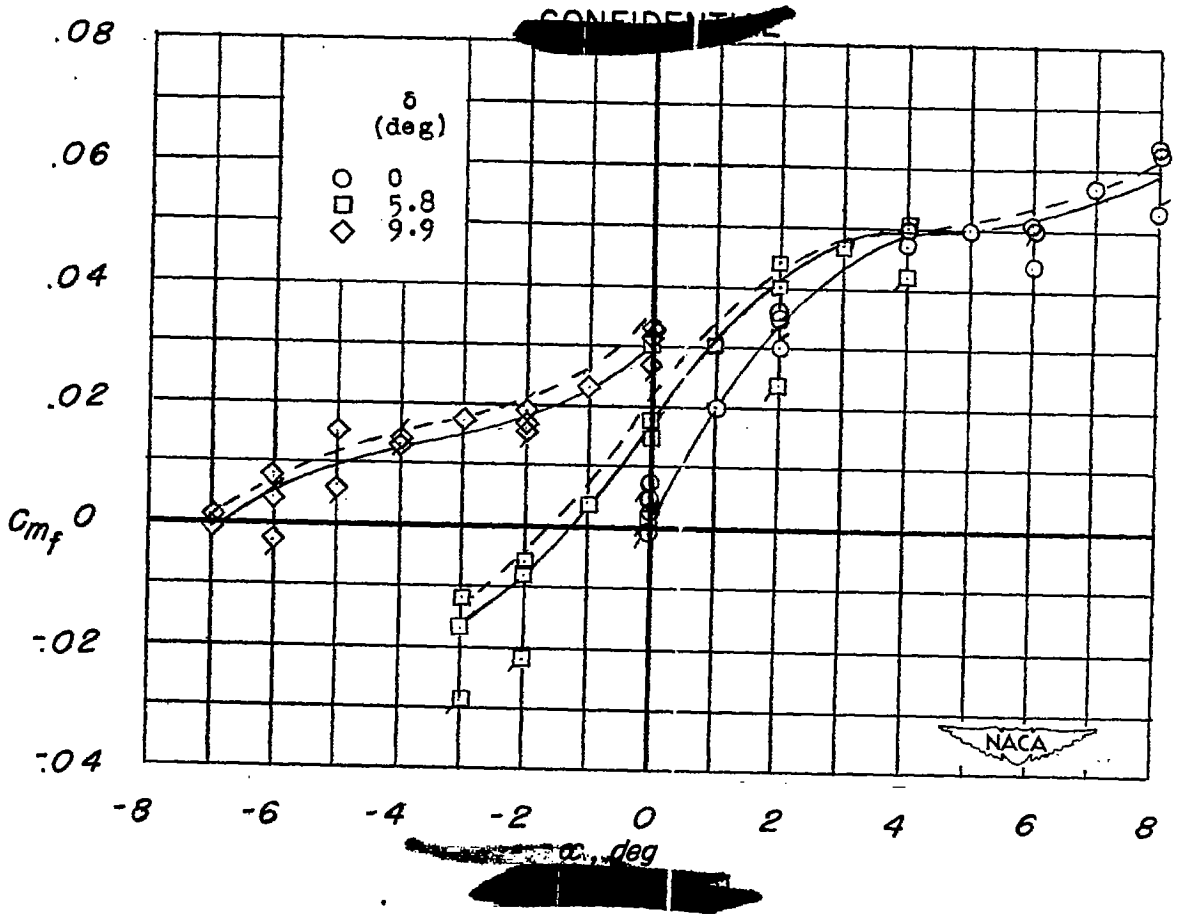

(b) C_{m_f} plotted against α.

Figure 7.– Concluded.

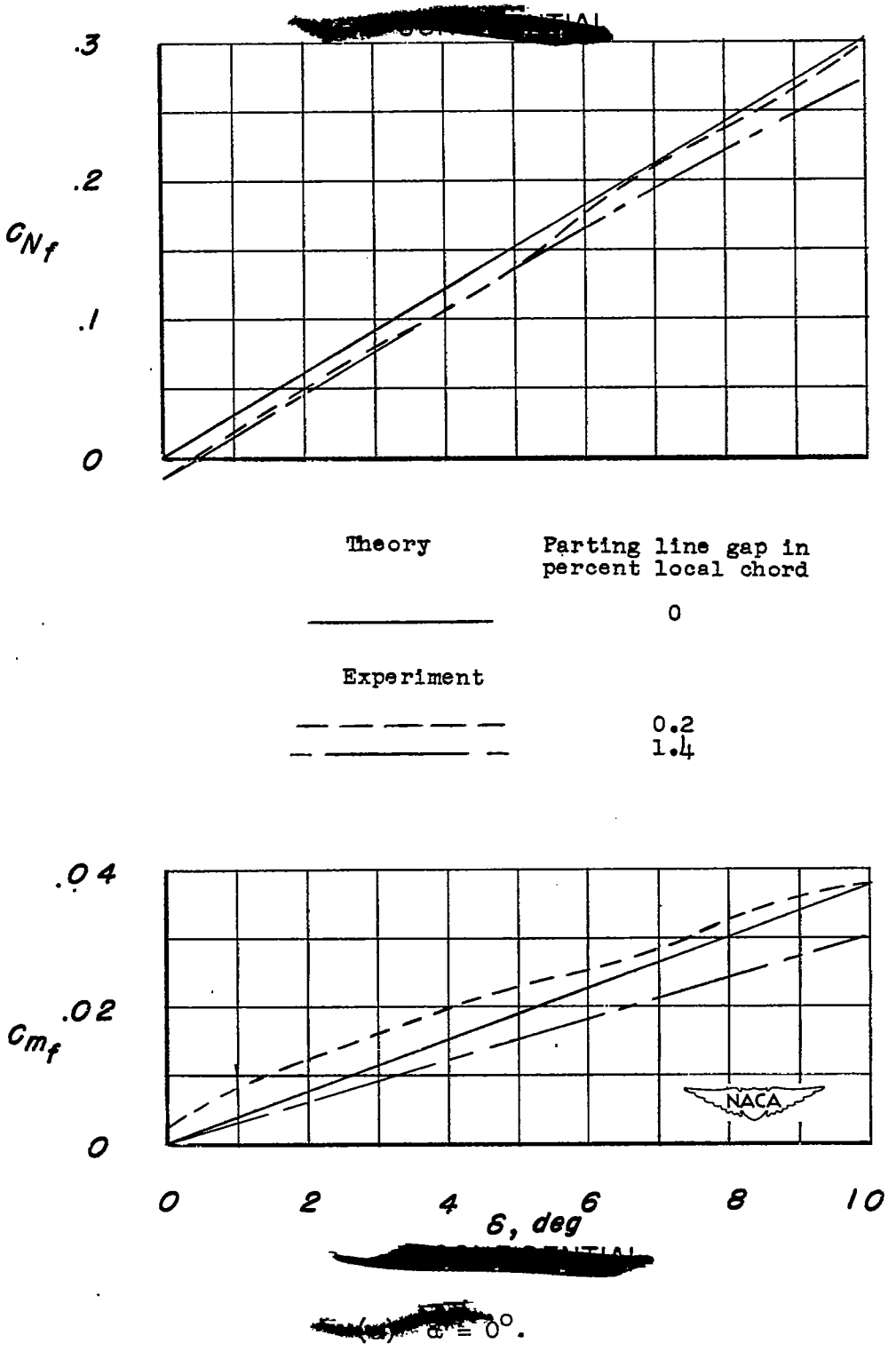

Figure 8.— Variation of aerodynamic loading characteristics with deflection of a tip control surface tested in presence of a semispan pointed wing. $R = 4.9 \times 10^6$; $M = 1.90$.

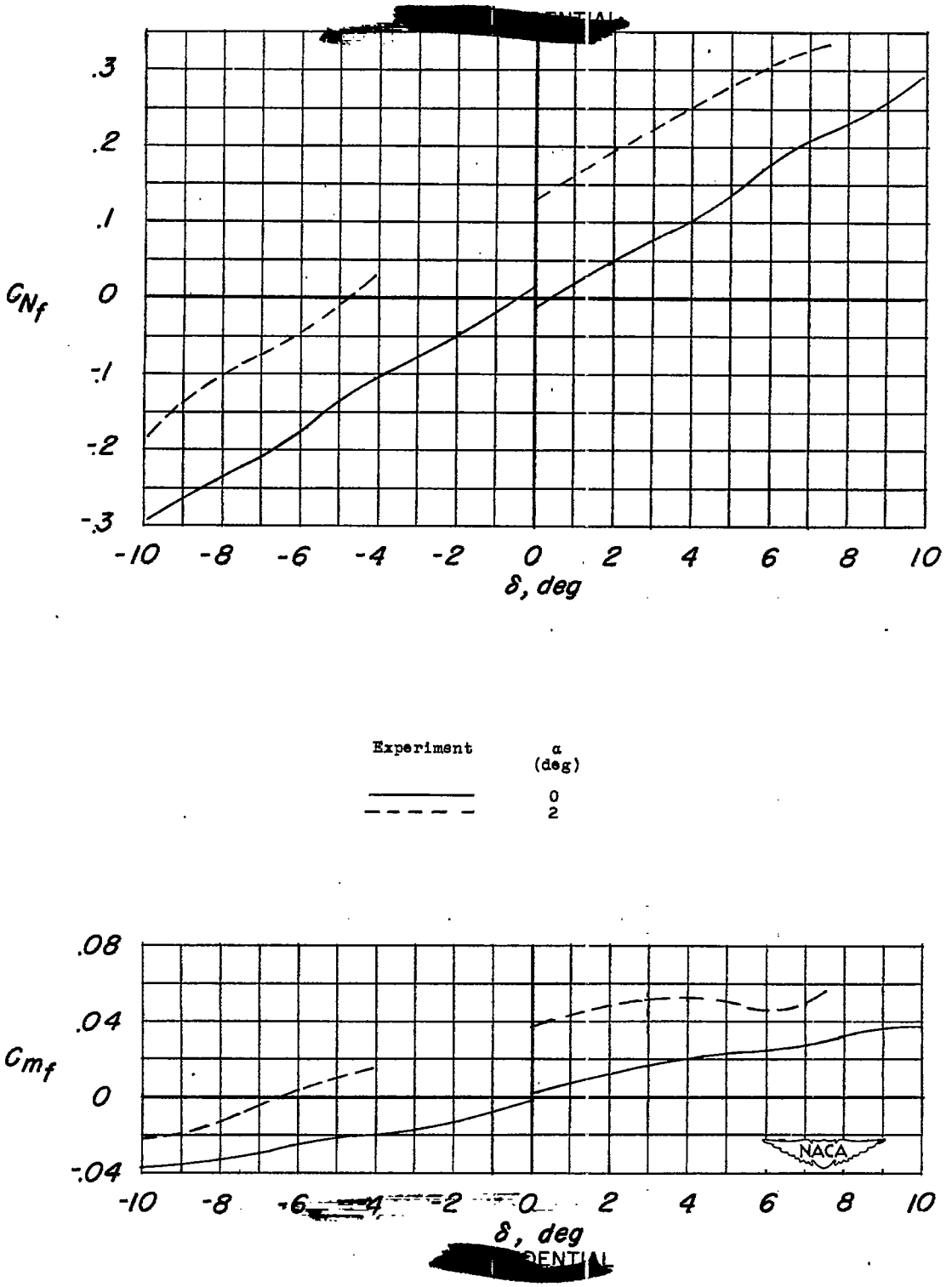

(b) $\alpha = 0^\circ$ and 2°. Parting line gap = 0.2 percent local chord.

Figure 8.– Concluded.